Comparative Molecular Field Analysis of Fungal Squalene Epoxidase Inhibitors

Vijay M. Gokhale and Vithal M. Kulkarni*

Pharmaceutical Division, Department of Chemical Technology, University of Mumbai, Matunga, Mumbai 400 019, India

Received May 28, 1999

Comparative molecular field analysis (CoMFA) of fungal squalene epoxidase inhibitors exhibiting antifungal activity reported in terms of minimum inhibitory concentration (MIC) was performed. Ninety-two molecules belonging to different chemical classes, namely terbinafine analogues, benzylamines, homopropargylamines, and carbon analogues were divided into training set and test set. The initial conformations of the inhibitors obtained from molecular dynamics simulations for 50 ps in aqueous solution were used in the study. Out of three charges used in the study, Gasteiger−Hückel charges result in models with good internal predictivity. Initial analysis of 92 molecules (analysis A) resulted in models with low predictive r^2 values for activity against three organisms. This data set was modified by exclusion of 13 molecules, and analysis was performed again. This analysis of 79 molecules (analysis B) resulted in improvement in predictivity of the CoMFA models and cross-validated r^2 values of 0.583, 0.509, and 0.502 for *Candida albicans, Aspergillus fumigatus,* and *Trichophyton mentagrophytes,* respectively. These models were used to predict the activities of the molecules belonging to the test set. The models from analysis B show better correlative and predictive properties than analysis A. Comparison of CoMFA contour maps for activity against three different fungi revealed differentiating structural requirements.

Introduction

Squalene epoxidase (EC 1.14.99.7) (SE) enzyme present in fungi and mammalian cell systems is involved in ergosterol biosynthesis.[1] Squalene epoxidase is a membrane bound enzyme and is involved in the conversion of squalene into squalene 2,3-epoxide, which is subsequently converted into lanosterol and further into ergosterol. Squalene epoxidase has been proven to be the target for the allylamine class of antifungal agents. This class of antifungal agents, mainly naftifine and terbinafine, exhibit antimycotic activity with widespread clinical applications.[2] Antifungal activity of allylamines has been attributed exclusively to the inhibition of the sterol biosynthetic pathway at the step of squalene epoxidation in fungi.

Squalene epoxidase enzyme system requires molecular oxygen, nicotinamide adenine dinucleotide phosphate (NADPH), and flavin adenine dinucleotide (FAD) for its activity.[3] Terbinafine and its analogues are found to be the potent inhibitors of fungal squalene epoxidase, and the potency is well correlated with the antifungal activity. Kinetic studies have shown that allylamines do not act as substrate analogues (squalene) at the enzyme interacting site and show noncompetitive kinetics.[4,5] It has been proposed that terbinafine and analogues interact or inhibit lipid-binding site on squalene epoxidase enzyme.

There are four different chemical classes of squalene epoxidase inhibitors developed over the years.[6−10] These are terbinafine analogues, benzylbenzylamine analogues, homopropargylamines, and terbinafine analogues lacking a central amino functional group, which have been tested against a variety of fungal pathogens. Important structural features of this class of inhibitors include fused aromatic or heteroaromatic systems, such as naphthyl or benzothiophenyl ring systems, and a typical "eneyne" system. In certain class of inhibitors this double- and triple-bonded system is replaced by benzyl or propargyl systems. Design of new potent inhibitors as antifungal agents is largely based upon structural information derived from the existing inhibitors. To study and deduce the correlation between structure and biological activity of these inhibitors, we have carried out a three-dimensional quantitative structure−activity relationship (3D-QSAR) study using comparative molecular field analysis (CoMFA).

CoMFA was proposed by Cramer et al. in 1988.[11] This methodology is applied to a set of molecules exhibiting biological activity with a similar mechanism of action. The molecules are superimposed based on a putative pharmacophore and are placed in a box of predetermined size. The steric and electrostatic interaction energies were calculated between each part of the molecule and a probe atom, usually an sp^3 carbon atom with +1.0 charge at lattice intersection points. These values are placed in a table containing values for biological activity. Using partial least squares (PLS) analysis, a number of components (latent variables) for describing variance in biological activity are determined. PLS is used to calculate cross-validated r^2 (r^2_{cv}) and conventional r^2 values. One of the advantages of CoMFA is the ability to predict the biological activity of the molecules and the representation of the relationship between steric/electrostatic property and biological activity in the form of contour maps.

* To whom correspondence should be addressed. E-mail: vithal@biogate.com.

10.1021/jm9806852 CCC: $18.00
Published on Web 12/04/1999

CoMFA has been applied in the study of enzyme inhibitors such as inhibitors of thermolysin,[12−14] renin,[12] angiotensin-converting enzyme,[13,14] human immunodeficiency virus-1 protease (HIV-1 PR),[15] HIV-1 integrase,[16] acetylcholinesterase,[17,18] human phospholipase A_2,[19] human DNA topoisomerase-I,[20] and interleukin-1β converting enzyme.[21] CoMFA study has been extended to receptor agonists and antagonists such as steroid receptor,[22] benzodiazepine receptor,[23] endothelin receptor,[24] melatonin receptor,[25] and adenosine receptors.[26] CoMFA study has also been applied to calcium entry blockers,[27] clodronic acid esters,[28] anticoccidial triazines,[29] cell growth inhibiting pyrazoloacridines,[30] antibody haptens,[31] anti-Picornavirus compounds,[32] and fused pyrazines with nematocide properties.[33] One of the most important input parameters in CoMFA is the "active conformation" and/or alignment of the molecules in three-dimensional space. Conformation of the molecules can be obtained from X-ray crystal structure and crystal structure in complex with the target enzyme, conformation derived through docking and NMR experiments, or active conformation derived from other 3D-QSAR techniques such as DISCO.[34]

In the present study, we have applied CoMFA method to derive 3D-QSAR between squalene epoxidase inhibitors and their antifungal activity against human fungal pathogens such as *Candida albicans*, *Aspergillus fumigatus*, and *Trichophyton mentagrophytes*. The initial analysis of 92 molecules (referred to as analysis A) resulted in CoMFA models with low correlative and predictive properties. This data set of 92 molecules was modified by exclusion of 13 molecules (carbon analogues) and were reanalyzed (analysis B). Results of these two analyses are presented here. Since no structural information is available for these classes of compounds, conformation of the molecules used in the present CoMFA study is obtained from molecular dynamics simulation of one molecule from each chemical class for 50 ps at 300 K in aqueous solution with water molecules added explicitly. This conformation was compared with the conformational data reported in the literature and used in the CoMFA study.[35]

We have analyzed the structural requirements of SE inhibitors in terms of steric/electrostatic field properties and compared the requirements for different fungal organisms. Such information is essential to understand the structure−activity relationship of squalene epoxidase inhibitors and subsequently for the design of potential antifungal agents.

Methods

Biological Activity. Ninety-two molecules belonging to various chemical classes such as allylamines, benzylbenzylamines, homopropargylamines, and carbon analogues have been reported as antifungals by the same research group.[6−10] Minimum inhibitory concentration (MIC) was determined with Sabouraud's dextrose broth (pH 6.5) for dermatophytes, aspergilli, and *S. schenckii* and malt extract broth (pH 4.8) for yeasts in glass tubes. The test compounds were dissolved in DMSO and serially diluted with the growth media. The growth control was read after 48 h (yeasts), 72 h (molds), and 7 days (*S. schenckii* and dermatophytes) incubation at 30 °C. The MIC was defined as the lowest concentration at which no signs of fungal growth were detectable macroscopically.[6]

Biological activity of these molecules in terms of minimum inhibitory concentration as log(1/MIC) against fungal species *Candida albicans*, *Aspergillus fumigatus*, and *Trichophyton mentagrophytes* was used in CoMFA study. In case of molecules where MIC values were not available as absolute values, the highest concentration tested was used as MIC value. It is necessary to evaluate the predictivity of the CoMFA models. This was achieved by dividing the molecules into training set and test set. Selection of training set and test set molecules was made by considering the fact that test set molecules represent range of biological activity and chemical classes similar to that of the training set. Thus the test set is the true representative of the training set.

Molecular Modeling. All molecular modeling and CoMFA studies were performed on a Silicon Graphics Indy R5000 computer. Structural manipulations were performed using Sybyl 6.22[36] with standard Tripos force field.[37]

The initial conformations of inhibitor molecules were obtained from molecular dynamics (MD) simulations in aqueous solution. The inhibitor molecules were solvated by a monolayer of water molecules within a precomputed box. Molecular dynamics simulation was carried out for 50 ps at 300 K. Inhibitor molecules were extracted from the lowest potential energy frame and were minimized till root-mean-square deviation 0.01 kcal/mol Å was achieved. Molecular dynamics simulations were performed on model inhibitors **16**, **35**, **48**, and **60** (terbinafine) (Chart 1). All other molecules were constructed using standard geometries and standard bond lengths starting from the nearest structure used in MD simulations (Chart 2). These molecules were minimized by conjugate gradient minimization algorithm till root-mean-square (rms) deviation 0.01 kcal/mol Å was achieved. A distance-dependent dielectric of 1.00 was used throughout the calculation.

Three different partial atomic charges were considered in CoMFA study. Empirical atomic charges were calculated using the Gasteiger−Hückel method, and semiempirical charges were calculated using AM1[38] and MNDO Hamiltonian[39] within MOPAC 6.00[40] (keywords 1scf, rhf).

Alignment Rules. Superimposition of the molecules was carried out by the following three alignments.

Alignment 1: This was done by rms fitting of the atoms to the template molecule, terbinafine (Chart 3) by considering (a) a tertiary nitrogen atom (N12), (b) an atom at the point of attachment of the aromatic ring with the side chain (C1), (c) atoms at the points of fusion of aromatic rings (C9 and C10), (d) atoms on the aromatic rings (C3 and C6), and (e) a methyl group attached to a nitrogen atom (C13).

Alignment 2: In this case, alignment of the molecules was carried out by flexible fitting (multifit) of atoms of the molecules to the template molecule, terbinafine. This involved energy calculations and fitting onto the template molecule by applying force (force constant = 20 kcal/mol Å) and subsequent energy minimization.

Alignment 3: This was carried out by using the SYBYL QSAR rigid body field fit command within SYBYL and using terbinafine as template molecule. Field fit adjusts the geometry of the molecules such that its steric and electrostatic fields match the fields of the template molecule.

CoMFA Interaction Energies. CoMFA steric and electrostatic interaction fields were calculated at each lattice intersection point of a regularly spaced grid of 2.0 Å. The CoMFA region was defined automatically which extended beyond the van der Waals volume of all molecules in *X*, *Y*, and *Z* directions. The van der Waals potential and Coulombic term, which represent the steric and electrostatic term, were calculated using standard TRIPOS force field. A distance-dependent dielectric constant of 1.00 was used. An sp^3 carbon atom with a van der Waals radius of 1.52 Å and +1.00 charge was used as probe atom. The steric and electrostatic fields were truncated at +30.0 kcal/mol, and the electrostatic fields

Chart 1. Structures of the Molecules Belonging to the Training Set[a]

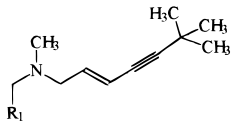

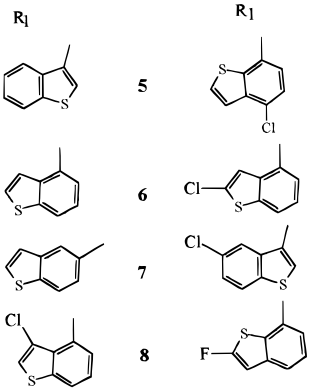

	R_1		R_1
1		**5**	
2		**6**	
3		**7**	
4		**8**	

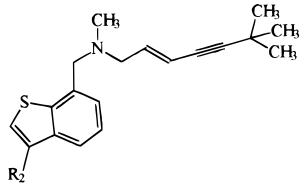

	R_2
9	-F
10	-CN
11	-CHO

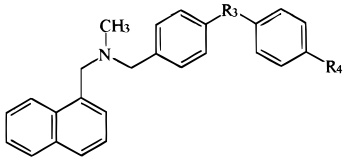

	R_3	R_4		R_3	R_4
12	-CH=CH-	-H	**16**	-C((CH$_3$)$_2$)-	-H
13	-CO-	-H	**17**	-C((CH$_3$)$_2$)-	-CH$_3$
14	-C(=CH$_2$)-	-H	**18**	-C(CH$_2$CH$_2$)-	-H
15	-CH$_2$-	-H	**19**	-N(COCH$_3$)-	-H
			20	-N(CH$_2$CH$_3$)-	-H

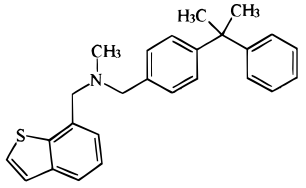

21

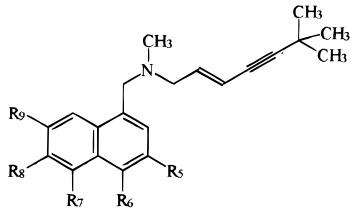

	R_5	R_6	R_7	R_8	R_9		R_5	R_6	R_7	R_8	R_9
22	-CN	-H	-H	-H	-H	**28**	-H	-H	-CH$_3$	-H	-H
23	-CH$_3$	-H	-H	-H	-H	**29**	-H	-H	-H	-F	-H
24	-H	-F	-H	-H	-H	**30**	-H	-H	-H	-H	-Cl
25	-H	-CN	-H	-H	-H	**31**	-H	-H	-H	-H	-CH$_3$
26	-H	-H	-F	-H	-H	**32**	-H	-H	-F	-H	-F
27	-H	-H	-Br	-H	-H						

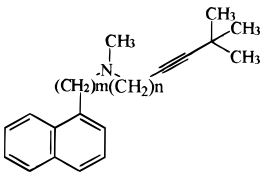

	m	n		m	n
33	1	3	**35**	2	1
34	2	2	**36**	1	1

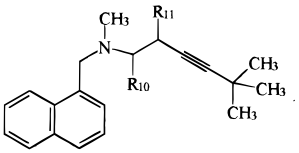

	R_{10}	R_{11}
37	-CH$_3$	-H
38	-H	-CH$_3$

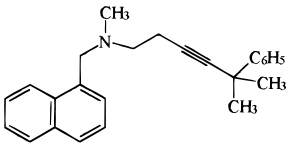

39

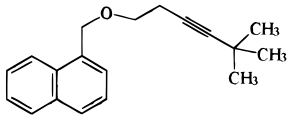

40

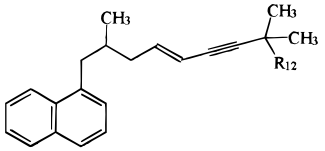

	R_{12}		R_{12}
41 *	-COOCH$_3$	**46 ***	-OH
42 *	-COOH	**47 ***	-NH$_2$
43 *	-CH$_2$OH	**48 ***	-NHCOCH$_3$
44 *	-CONH$_2$	**49 ***	-N(CH$_3$)$_3$
45 *	-CN	**50 ***	-N(CH$_3$)(C$_6$H$_5$)

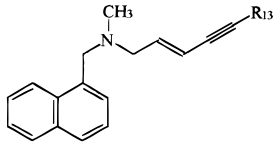

	R_{13}		R_{13}
51		**56**	
52		**57**	-C((CH$_3$)$_2$)OH
53		**58**	-C((CH$_3$)$_2$)OCH$_3$
54	-C(=CH$_2$)CH$_3$	**59**	-I
55	-C(=CH$_2$)C(CH$_3$)$_3$	**60**	-C(CH$_3$)$_3$ (terbinafine)

[a] Structures marked with an asterik (*) are excluded in analysis B.

Chart 2. Structures of the Molecules Belonging to Test Set[a]

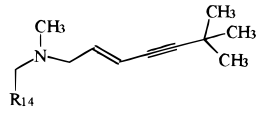

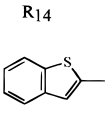

61

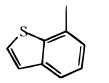

62

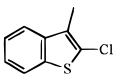

63

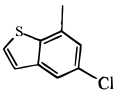

64

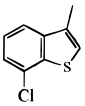

65

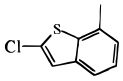

66

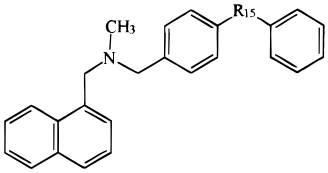

	R_{15}
72	(bond)
73	-O-
74	-NH-

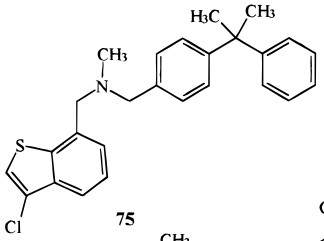

75

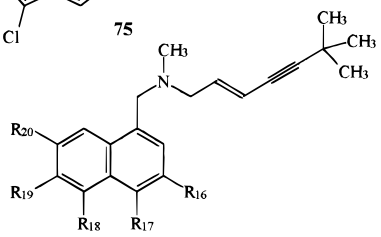

	R_{16}	R_{17}	R_{18}	R_{19}	R_{20}
76	-F	-H	-H	-H	-H
77	-H	$-CH_3$	-H	-H	-H
78	-H	-H	-Cl	-H	-H
79	-H	-H	-CN	-H	-H
80	-H	-H	-H	-F	-H
81	-H	-H	-H	-H	-F

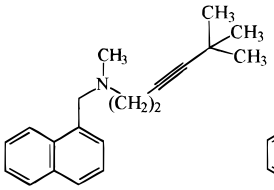

82

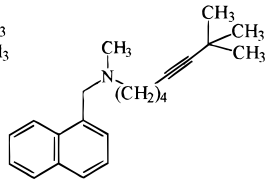

83

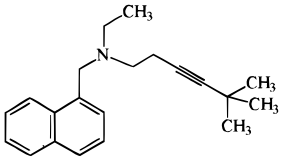

84

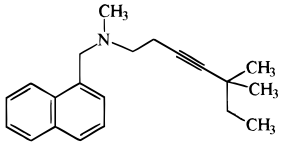

85

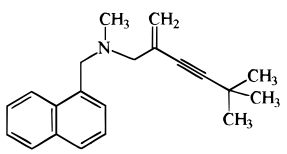

86

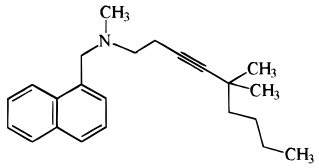

87

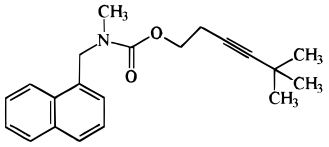

88

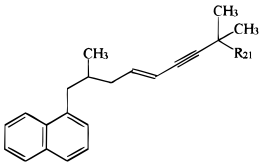

	R_{21}
89 *	$-CONHCH_3$
90 *	$-CH_2NH_2$
91 *	$-NHCOCH_3$

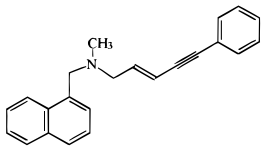

92

[a] Structures marked with an asterik (*) are excluded in analysis B.

were ignored at the lattice points with maximal steric interactions.

Partial Least Squares (PLS) Analysis. Partial least squares was used in conjunction with the cross-validation option to determine the optimum number of components which were then used in deriving the final CoMFA model without cross-validation. The results from cross-validation analysis were expressed as the cross-validated r^2 value (r^2_{cv}). The cross-

Chart 3. Terbinafine Molecule with Atoms Used for Superimposition Are Marked

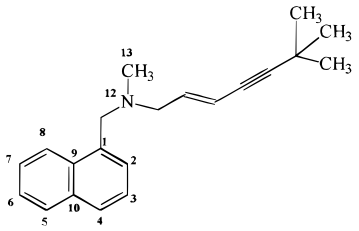

validated r^2 is defined as

$$r^2_{cv} = 1 - \frac{\text{PRESS}}{\sum(Y - Y_{mean})^2}$$

where PRESS $= \sum(Y - Y_{pred})^2$.

The number of components that result in highest cross-validated r^2 and lowest standard error of predictions (s) were taken as the optimum number of components. Cross-validation was performed using leave-one-out (LOO) method in which one compound is removed from the data set and its activity is predicted using the model derived from the rest of the data set. LOO cross-validation was carried out with the number of components set equal to 10. Cross-validation was also performed by using group technique in which the number of groups equal to two (leave-half-out) was used. In this case compounds of the data set are randomly divided into two groups, and the activity of the compounds from one group are predicted using the model derived from the other group. The process of group cross-validation was performed 100 times. The final r^2_{cv} value was calculated by taking the mean of 100 runs. Cross-validated r^2 values obtained from both leave-one-out and leave-half-out were compared for each PLS analysis.

Equal weights were assigned to steric and electrostatic fields using COMFA_STD scaling option. To speed up the analysis and reduce noise, a minimum filter value "σ" of 2.0 kcal/mol was used. Final analysis was performed to calculate the conventional r^2 value with a number of cross-validation groups set to zero using the optimum number of components. To further assess the robustness and statistical confidence of the derived models, bootstrapping analysis (100 runs) was performed. To check for chance correlation, PLS analysis was performed by randomization of the biological activity. This was done by randomly changing biological activity data and performing PLS analysis to calculate the cross-validated r^2 value. The process was repeated 100 times.

Predictive r^2 Value. To validate the derived CoMFA models, biological activities of the test set molecules were predicted using models derived from training set.

Predictive r^2 value was calculated using formula

$$r^2_{\text{predictive}} = \frac{\text{SD} - \text{PRESS}}{\text{SD}}$$

where SD is the sum of squared deviation between the biological activity of the test set molecule and the mean activity of the training set molecules and PRESS is the sum of squared deviations between the actual and the predicted activities of the test set molecules.

Calculation of Extrapolation Values. We have calculated the percent extrapolation values (% extrapolation) from the QSAR>ANALYSIS>PREDICT command from SYBYL for each test set predictions using both the analyses. These values were calculated as follows

$$\text{percent extrapolation} = \frac{\text{number of terms extrapolated}}{\text{number of terms considered for predictions}} \times 100$$

Calculation of Additional Descriptors. Different types of physicochemical descriptors were calculated using Cerius2 version 3.5[41] running on a Silicon Graphics O2 R5000 workstation. The molecules under study were directly imported from SYBYL. Charges were assigned to the molecules using the Gasteiger method within Cerius2. Various types of descriptors were calculated. These included electronic descriptors, spatial descriptors, structural descriptors, thermodynamic descriptors, and calculated logP (ClogP) values.[42] These descriptors were directly used in the PLS analysis.

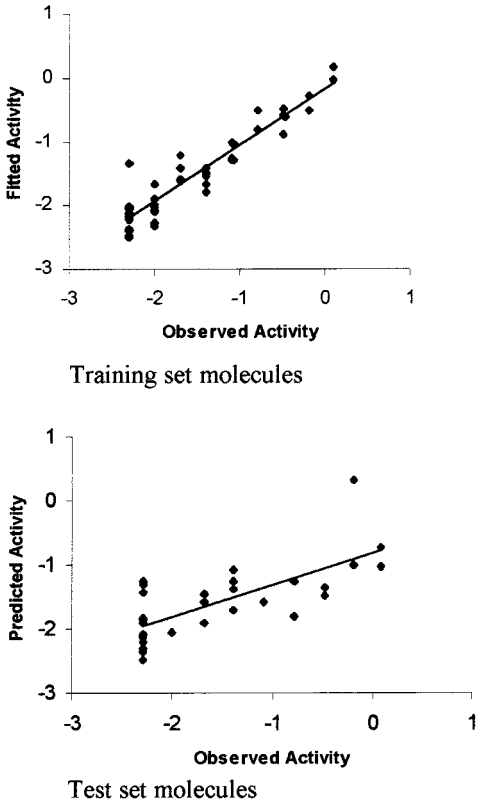

Figure 1. Graph of observed activity versus fitted/predicted activity for *C. albicans* (analysis B), activity expressed as log-(1/MIC) with MIC in terms of mg/L.

Results and Discussion

Three different types of antifungal activity data reported in terms of minimum inhibitory concentration (MIC) values against human pathogenic, namely *C. albicans*, *A. fumigatus*, *T. mentagrophytes*, were used (Figures 1−3).

All the cross-validated results were analyzed by considering the fact that a value of r^2_{cv} above 0.300 indicates that the probability of chance correlation is less than 5%.[43]

Conformation of the molecules used in the study was obtained by molecular dynamics simulations for 50 ps at 300 K in aqueous solution with water molecules added explicitly. Relative alignment of the molecules was then carried out by using three techniques, namely rms fitting, multifit (flexible fitting), and SYBYL QSAR rigid body field fit.

Analysis of 92 molecules (analysis A) comprising training set (60 molecules) and test set (32 molecules) resulted in models with low cross-validated r^2 values and poor predictivity. This data set of 92 molecules was modified by exclusion of 13 molecules from the analysis, and a data set of 79 molecules (training set 50 molecules and test set 29 molecules) was obtained. The molecules belonging to the class of carbon analogues were excluded

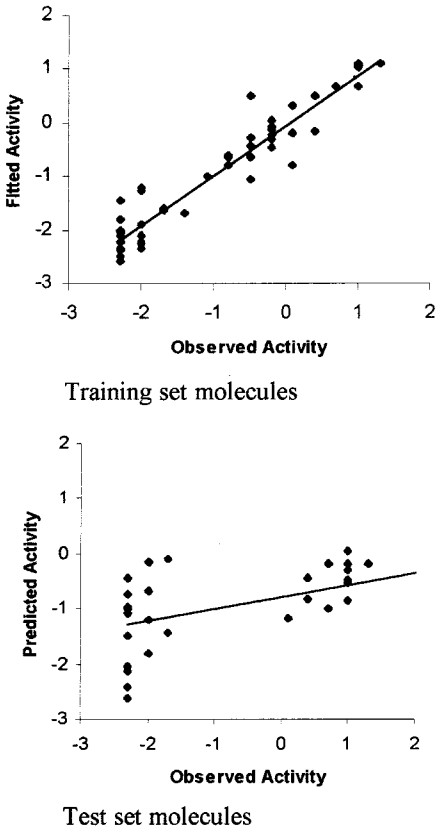

Figure 2. Graph of observed activity versus fitted/predicted activity for *A. fumigatus* (analysis B), activity expressed as log(1/MIC) with MIC in terms of mg/L.

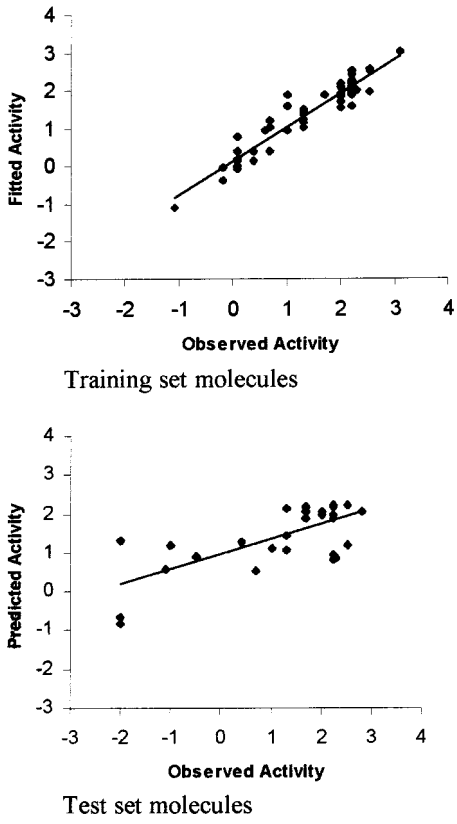

Figure 3. Graph of observed activity versus fitted/predicted activity for *T. mentagrophytes* (analysis B), activity expressed as log(1/MIC) with MIC in terms of mg/L.

from the data set as most of these molecules have different pK_a values and, hence, can exhibit different physicochemical properties than the rest of the data set. This difference in the chemical nature of these molecules forms the basis for their exclusion. This data set was reanalyzed (analysis B). Analysis B showed improvement in correlative and predictive properties. A preliminary study was made to assess the effects of charges (data not shown), and the results indicate that the models with Gasteiger−Hückel charges show better internal predictivity and better non-cross-validated r^2 values. Superimposition of the molecules was carried out using three different alignments. Alignment 1, i.e., rms fitting of atoms, shows better r^2 values than the other two alignments.

To make a comparison between CoMFA analysis and contour maps for activity against three fungal organisms, all the molecules were assigned Gasteiger−Hückel charges. Results of CoMFA analysis A and analysis B are presented in Tables 1 and 3, respectively. Cross-validation analysis was also performed by the leave-half-out technique. In case of leave-half-out, molecules are randomly divided into two groups, and a model derived from one group is used to predict the activities of the molecules belonging to other group. Final r^2_{cv} value was calculated by taking the average of 100 runs. Although this average cross-validated r^2 value was less than the leave-one-out r^2_{cv} value, in some cases the values were higher, reflecting the inconsistency in the data set. Results of leave-half-out cross-validation and randomization are presented in Tables 2 and 4 for analysis A and B, respectively.

CoMFA for Activity against *C. albicans*. Results of analysis A using Gasteiger−Hückel charges and alignment 1 are presented in Table 1. Results show that the model for activity against *C. albicans* exhibits a cross-validated r^2 value of 0.394 with seven components. A conventional r^2 value of 0.953 and an F value 152.141 was obtained. The model yielded a high r^2 value of 0.976 during bootstrapped analysis.

Analysis B (Table 3) of activity against *C. albicans* exhibits a cross-validated r^2 value of 0.583, when ClogP was added as an additional descriptor with an optimum number of components of four. A high conventional r^2 value of 0.893 and F value 93.58 was obtained. A high r^2 value of 0.919 during 100 runs of bootstrapped analysis further supports the statistical validity of the model. The cross-validated r^2 value of 0.455 during leave-half-out analysis further supports the validity of the model. Contributions of steric and electrostatic fields were 39.4% and 53.2%. The results of analysis B models show improvement in correlative properties over analysis A.

CoMFA for Activity against *A. fumigatus*. Analysis A resulted in a cross-validated r^2 value of 0.345 and a conventional r^2 value of 0.893 with an F value = 73.40. A high r^2 value of 0.945 during 100 runs of bootstrapped analysis was obtained. Analysis B shows that the model derived from alignment 1 resulted in a cross-validated r^2 value of 0.509 with the optimum number of components equal to five. This model exhibited a very high conventional r^2 value of 0.918 and an F value = 98.39. The high r^2 value of 0.951 during 100 runs of bootstrapping analysis further supports robustness and statistical

Table 1. Summary of CoMFA Results (Analysis A)

	C. albicans			*A. fumigatus*			*T. mentagrophytes*		
alignments	1	2	3	1	2	3	1	2	3
r^2_{cv}	0.394	0.338	0.279	0.345	0.299	0.167	0.533	0.588	0.512
SEP	0.569	0.595	0.588	0.949	0.991	1.023	0.922	0.899	0.989
r^2_{conv}	0.953	0.958	0.506	0.893	0.933	0.272	0.894	0.977	0.988
std error	0.158	0.151	0.487	0.384	0.306	0.956	0.440	0.213	0.155
no. of comp.	7	7	8	6	7	1	4	8	9
F value	152.14	167.38	59.32	73.40	103.82	27.62	115.43	270.59	439.94
$P_{r2=0}$	0.00	0.00	0.00	0.00	0.00	0.00	0.00	0.00	0.00
contribution									
steric	42.3	45.3	33.5	44.9	45.8	34.6	40.9	45.0	42.8
electrostatic	57.7	54.7	66.5	55.1	54.2	65.4	59.1	55.0	57.2
r^2_{pred}	0.437	0.331	0.235	−0.148	−0.189	−0.06	−0.107	0.023	−0.062
r^2_{bs}[a]	0.976	0.975	0.513	0.945	0.966	0.327	0.940	0.990	0.994
std dev[a]	0.010	0.011	0.132	0.023	0.013	0.147	0.022	0.005	0.003

[a] Results from 100 runs of bootstrapped analysis.

Table 2. Results of Analysis with Randomized Biological Activities and Leave-Half-Out Cross-Validation (Analysis A)

	r^2_{cv}[a]			r^2_{cv}[b]		
	C.a.[c]	*A.f.*[c]	*T.m.*[c]	*C.a.*[c]	*A.f.*[c]	*T.m.*[c]
mean	0.231	0.199	0.493	−0.105	−0.082	−0.074
std dev	0.133	0.100	0.051	0.166	0.109	0.151
high	0.491	0.388	0.562	0.309	0.271	0.294
low	−0.051	0.016	0.388	−0.965	−0.531	−0.589

[a] Leave-half-out with optimum number of components average of 25 runs. [b] Cross-validated r^2 with randomized biological activity average of 100 runs. [c] *C.a.*: *C. albicans* model with alignment 1 and Gasteiger−Hückel charges. *A.f.*: *A. fumigatus* model with alignment 1 and Gasteiger−Hückel charges. *T.m.*: *T. mentagrophytes* model with alignment 2 and Gasteiger−Hückel charges.

Table 3. Summary of CoMFA Results[a] (Analysis B)

	C. albicans		*A. fumigatus*		*T. mentagrophytes*	
	CoMFA	CoMFA ClogP	CoMFA	CoMFA ClogP	CoMFA	CoMFA ClogP
r^2_{cv}	0.522	0.583	0.509	0.464	0.502	0.517
SEP	0.532	0.496	0.849	0.897	0.700	0.697
r^2_{conv}	0.902	0.893	0.918	0.925	0.903	0.914
SE	0.241	0.252	0.347	0.336	0.308	0.294
no. of comp.	4	4	5	6	4	5
F value	103.69	93.58	98.39	88.23	105.02	93.38
$P_{r2=0}$	0.00	0.00	0.00	0.00	0.00	0.00
contributions						
steric	39.3	39.4	40.0	38.4	40.7	42.2
electrostatic	60.7	53.2	60.0	59.0	59.3	55.9
ClogP		7.5		2.6		1.9
r^2_{pred}	0.489	0.542	0.331	0.335	0.452	0.436
r^2_{bs}[b]	0.944	0.919	0.951	0.962	0.940	0.947
std dev[b]	0.019	0.024	0.020	0.014	0.021	0.018

[a] Gasteiger−Hückel charges and alignment 1 (rms fitting). [b] Results from 100 runs of bootstrapped analysis.

validity of the model. Steric and electrostatic fields contributed 40% and 60%, respectively.

CoMFA for Activity against *T. mentagrophytes*. In the case of analysis A, superimposition of the molecules with rms fitting resulted in an r^2_{cv} value of 0.533, and flexible fitting yielded an r^2_{cv} value of 0.588 with eight number of components. Thus better internal predictivity was obtained with alignment 2. Analysis B shows that superimposition of the molecules with rms fitting resulted in a model with a cross-validated r^2 value of 0.502 with number of components equal to four. A conventional r^2 value of 0.903 and *F* value = 105.03 was obtained for this model. Relative contributions of steric and electrostatic fields were 40.7% and 59.3%, respectively. Leave-half-out r^2_{cv} of 0.388 further supports the validity of the model.

Table 4. Results of Analysis with Randomized Biological Activities and Leave-Half-Out Cross-Validation[a] (Analysis B)

	r^2_{cv}[b]			r^2_{cv}[c]		
	C.a.[d]	*A.f.*[d]	*T.m.*[d]	*C.a.*[d]	*A.f.*[d]	*T.m.*[d]
mean	0.455	0.250	0.388	−0.075	−0.154	−0.170
std dev	0.118	0.129	0.093	0.096	0.143	0.156
high	0.662	0.589	0.538	0.143	0.337	0.147
low	0.073	0.003	0.093	−0.417	−0.578	−0.663

[a] Gasteiger−Hückel charges and rms fitting. [b] Leave-half-out with optimum number of components average of 100 runs. [c] Cross-validated r^2 with randomized biological activity average of 100 runs. [d] *C.a.*: *C. albicans* model. *A.f.*: *A. fumigatus* model. *T.m.*: *T. mentagrophytes* model.

Thus, in the case of all three organisms, analysis of the modified data set (analysis B) shows improvement in predictive and correlative properties over analysis A.

We have used additional descriptors in analysis of 79 molecules to account for the extrapolation required better predictions.

Use of Additional Descriptors. Activity data used in the present study is in vitro data (cell-based assays), and such a type of activity data could have contributions not only from steric and electrostatic fields but also other physicochemical properties. These properties account for the transport phenomenon and pharmacokinetic profiles of the molecules.

To account for the lipophilic properties, which influence this type of activity, ClogP was included in the analysis. In the case of analysis B, ClogP contributed significantly to CoMFA models. In the case of *C. albicans*, ClogP contribution is 7.5% and this inclusion has improved the cross-validated r^2 from 0.522 to 0.583.

We have also calculated various descriptors using Cerius2 software and used in analysis B. These descriptors included electronic descriptors (such as superdelocalizability, dipole moment, atomic polarizabilities, HOMO and LUMO energies), spatial descriptors (molecular surface area, molecular volume, molecular density), structural descriptors (molecular weight, number of rotatable bonds), and thermodynamic descriptors (desolvation free energies, molar refractivity). These descriptors were calculated and directly used as additional regressors in the PLS analysis. Inclusion of these descriptors did not improve the predictivity of the models.

In the case of *C. albicans*, inclusion of any of these descriptors does not result in r^2_{cv} better than 0.583. Molar refractivity (MR) along with ClogP results in r^2_{cv}

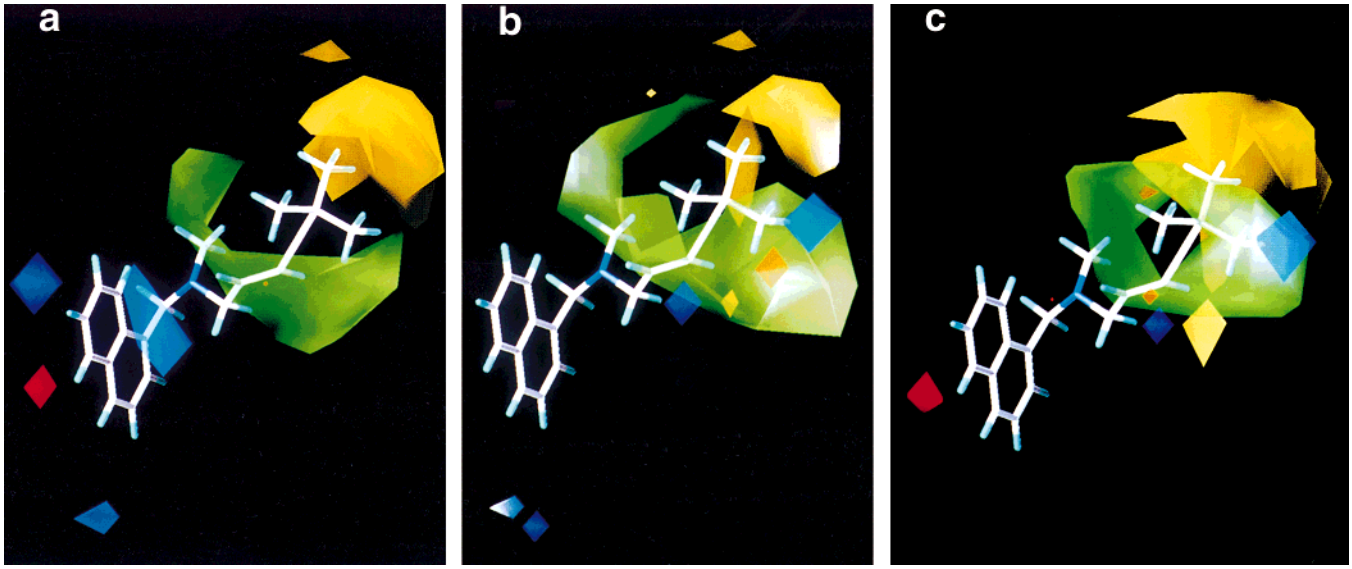

Figure 4. CoMFA steric and electrostatic stddev * coeff contour plot from analysis B for activity against (a) *C. albicans*, (b) *A. fumigatus*, and (c) *T. mentagrophytes* with terbinafine. Sterically favored areas (contribution level 80%) are shown as green polyhedra; sterically disfavored areas (contribution level 20%) are shown as yellow polyhedra. Positive charge favored areas (contribution level 80%) are shown as blue polyhedra; negative charge favored areas (contribution level 20%) are shown as red polyhedra.

of 0.565, but resultant model shows lower F value of 76.8. Model with superdelocalizability (Sr) shows r^2_{cv} of 0.509, and the contribution of Sr is insignificant (about 0.5%). In the case of *A. fumigatus*, none of these externally added descriptors result in better correlative and internally predictive models. Similar results are observed in the case of *T. mentagrophytes* models.

Analysis of Contour Maps. Contour maps were generated for analysis B for activity against fungal organisms. Contour maps were generated as scalar products of coefficients and standard deviation associated with each CoMFA column. We have discussed contour maps for activity against each organism with respect to analysis B.

Analysis of Contour Maps for Activity against *C. albicans*. CoMFA contour maps generated for activity against *C. albicans* are depicted in Figure 4a. Analysis shows that steric fields are mainly concentrated around the side chain of the molecules (*tert*-butyl group in terbinafine). A large sterically favorable green region is observed around the terminal end of the molecules. Molecules containing bulky groups such as *tert*-butyl exhibit better activity against *C. albicans*. This green region is accompanied by the sterically forbidden yellow region above the triple-bonded functionality. Thus the rigidity provided by the triple bond seems to be important for activity. The orientation of bulky side chain plays an important role in the activity. Molecules **12**, **13**, and **14** exhibit less activity since the bulky phenyl ring extends into the yellow region.

Electrostatic fields are mainly observed around the fused aromatic ring system of the molecule. A red region is observed around the C_5/C_6 substituent. Thus the substitution of an electronegative atom or group imparts enhanced activity as in the case of molecule **9** (fluoro group). The presence of a blue region above the aromatic ring signifies the importance of electron withdrawing groups, and the sulfur atom in benzothiophene ring results in better activity than the corresponding naphthyl analogue. Molecule **9** shows 4 times better activity than the corresponding naphthyl analogue, molecule **26**. Another blue region is also seen around the C_3/C_4 substituent. The presence of an electropositive group seems to favor the activity.

Analysis of Contour Maps for Activity against *A. fumigatus*. Contour maps generated for activity against *A. fumigatus* are shown in Figure 4b. Steric fields are observed around the side chain of the molecules. A large sterically favorable green region is observed around the *tert*-butyl group. This green region is accompanied by a sterically forbidden yellow region, indicating strict conformational requirements around the side chain. Molecules having a bulky flexible side chain due to the absence of structurally rigid elements show reduced activity. Electrostatic fields are observed around fused aromatic ring systems. A relatively small red region is observed around C_5/C_6 substituents, indicating the presence of electronegative atoms at these positions favorable for activity. A blue region is observed around C_3/C_4 substituents on fused aromatic ring systems. Thus the presence of groups such as methyl ($-CH_3$) at C_3 in the case of molecule **23** exhibits better activity than molecule **22** ($-CN$ at C_3). A red region is also seen around the terminal end of the molecules.

Analysis of Contour Maps for Activity against *T. mentagrophytes*. Figure 4c shows the contour maps generated for *T. mentagrophytes*. As seen in the case of *C. albicans* and *A. fumigatus*, a steric region is observed around the terminal end of the molecule. Sterically favorable green region is seen around the *tert*-butyl group of the side chain. This green region is accompanied by sterically forbidden yellow region, but in this model the yellow region is seen beyond the green region and not above the triple-bonded functionality. Thus there appears a strict structural requirement around the side chain. Molecule **56** having extended side

chain with acetylenic groups shows low activity since *tert*-butyl groups protrude into the yellow region. Electrostatic regions are observed around the fused aromatic ring system. A red region is seen around the C_5/C_6 substituent as seen in the case of models for *Candida sp.* and *Aspergillus sp.* The presence of electronegative atoms at these positions (fluoro in molecule **9**) results in better activity. A blue region is observed beyond the steric regions in the end part of the molecules.

Comparison of CoMFA Contour Maps. CoMFA contour maps generated for activity against different fungal organisms were compared so as to understand common structural features required for activity.

One of the most important common features in all three models is the presence of a large sterically favorable green region around the *tert*-butyl group of the molecules. This green region signifies the importance of a sterically bulky group in the side chain for better activity. This green region is always accompanied by a yellow region. Both these regions impose strict structural requirements for the side chain in the molecules. The sterically forbidden yellow region is present above the triple-bonded functionality in the case of models developed for *C. albicans* and *A. fumigatus*, indicating rigid conformational requirements. But in the case of the *T. mentgrophytes* model, this yellow region is seen beyond the green region and any bulky substituent extending beyond the green region leads to reduced activity. In the case of the *T. mentagrphytes*, structural requirements are more rigid than the other two organisms. An electronegative favorable red region is seen around the C_5/C_6 position on the fused aromatic ring system. Thus the presence of an electronegative group at these positions seems to impart better activity.

One of the distinguishing features in the case of the *C. albicans* model is the presence of a blue region above aromatic rings. The presence of an electron withdrawing group and a sulfur atom in the benzothiophene ring system result in better activity than naphthyl ring analogues.

Predictivity of the Models. Predictivity of the models was evaluated by predicting the activity of the molecules belonging to the test set. Predictive power was expressed as predictive r^2 values. Results obtained from analysis A and analysis B are summarized in Tables 1 and 3, respectively.

In the case of analysis A, the model for activity against *C. albicans* was able to predict the activities of the test set satisfactorily, and the predictive r^2 value of 0.437 was obtained. But with the exclusion of 13 compounds from the data set, reanalysis (analysis B) resulted in a better predictive r^2 value of 0.542. In the case of analysis A for *A. fumigatus*, a low predictive r^2 value of -0.148 was obtained, and analysis B shows a predictive r^2 value of 0.331. For *T. mentagrophytes*, analysis A shows a low predictive r^2 value of 0.023, while with analysis B predictions for test set molecules were moderately good and a predictive r^2 value of 0.452 was obtained.

Additional descriptors were used to parametrize for the transport phenomenon and other factors, which play an important role in such type of activity data. Only in the case of *C. albicans* with analysis B did ClogP contribute significantly to the activity, and a better predictive r^2 value was obtained with ClogP. Inclusion of other descriptors resulted either in a decrease in predictivity or the contribution was not significant for analysis B. For *C. albicans*, the model with inclusion of molar refractivity (MR) resulted in a predictive r^2 value of 0.481. In the case of *A. fumigatus* and *T. mentagrophytes*, inclusion of these descriptors resulted in models with low cross-validated r^2 and a decrease in overall predictivity.

Results indicate that exclusion of some compounds from the original data set of 92 molecules (analysis A) resulted in a modified data set (analysis B) with better correlative and predictive properties.

We have calculated the percent extrapolation values (% extrapolation) required for test set predictions using both analysis A and B (see Table 2 of Supporting Information). The extrapolation required in both of the analyses for all three models are similar, suggesting that the information generated in analysis B is similar to that in analysis A. In certain cases, such as molecules **61**, **62**, and **64**, the extrapolation required in analysis A is more than in analysis B. However, in most of the cases the percent extrapolation value is below 3.0, supporting the moderate predictivity of the models.

Conclusion

Comparative molecular field analysis study of squalene epoxidase inhibitors as antifungals was aimed at deriving and comparing structural requirements for antifungal activity. A data set containing 92 molecules was divided into training set (60 molecules) and test set (32 molecules). Minimum inhibitory concentration (MIC) in mg/L against three different fungi was used as biological activity. Analysis of this data set containing 92 molecules (analysis A) resulted in CoMFA models with low predictivity. Further analysis by excluding 13 molecules (analysis B) resulted in CoMFA models with better correlative and predictive properties than analysis A. With inclusion of the lipophilicity descriptor, ClogP, values seem to contribute significantly to the models against *C. albicans*.

Predictive power of the derived models was assessed by predicting the activities of the test set molecules. Models obtained in analysis B show better predictivity than in analysis A. CoMFA models were able to predict the activities to a better extent, and moderately good predictions were obtained. Low predictions could be due to the fact that activity data available are approximate, and CoMFA fields alone were not sufficient to model the activity. In most of the cases the percent extrapolation value is below 3.0, supporting the moderate predictivity of the models.

The statistical results obtained from the present study are moderately predictive, and the structural information derived from this study can be utilized in the design of broad-spectrum antifungal agents.

Acknowledgment. Authors thank University Grants Commission (UGC), New Delhi, for financial support under its Department of Special Assistance (DSA) and COSIST programs. One of the authors (V.M.G.) is grateful to UGC for the award of a senior research fellowship. V.M.G. also thanks Santosh Kulkarni and Tanaji Talele for useful discussions and suggestions.

Supporting Information Available: Two tables containing observed and predicted activities of 92 molecules (Table 1) and the extrapolation values (Table 2) for test set predictions. This material is available free of charge via the Internet at http://pubs.acs.org.

References

(1) Ryder, N. S. Mode of Action of Allylamines. In *Sterol Biosynthesis Inhibitors- Pharmaceutical and Agrochemical Aspects*. Berg, D., Plempel, M., Eds.; VCH Publishers: Weinheim, 1988; p 151−167.

(2) Stutz, A. Allylamine Derivatives − A New Class of Active Substances in Antifungal Chemotherapy. *Angew. Chem., Int. Ed. Engl.* **1987**, *26*, 320−328.

(3) Ryder, N. S. Inhibition of Squalene Epoxidase and Sterol Side-Chain Methylation by Allylamines. *Biochem. Soc. Trans.* **1980**, *18*, 45−46.

(4) Ryder, N. S.; Dupont, M. Inhibition of Squalene Epoxidase by Allylamine Antimycotic Compounds − A Comparative Study of Fungal and Mammalian Enzymes. *Biochem. J.* **1985**, *230*, 765−770.

(5) Paltauf, F.; Daum, G.; Zuder, G.; Hogenauer, G.; Schulz, G.; Seidl, G. Squalene and Ergosterol Biosynthesis In Fungi Treated with Naftifine, A New Antimycotic Agent. *Biochim. Biophys. Acta* **1982**, *712*, 268−273.

(6) Nussbaumer, P.; Petranyi, G.; Stutz, A. Synthesis and Structure−Activity Relationships of Benzo[*b*]thienylallylamine Antimycotics. *J. Med. Chem.* **1991**, *34*, 65−73.

(7) Nussbaumer, P.; Dorfstatter, G.; Grassberger, M. A.; Leitner, I.; Meingasser, J. G.; Thirring, K.; Stutz, A. Synthesis and Structure−Activity Relationships of Phenyl-substituted Benzylamine Antimycotics: A Novel Benzylbenzylamine Antifungal Agent for Systemic Treatment. *J. Med. Chem.* **1993**, *36*, 2115−2120.

(8) Nussbaumer, P.; Dorfstatter, G.; Leitner, I.; Mraz, K.; Vylpel, H.; Stutz, A. Synthesis and Structure−Activity Relationships of Naphthalene-Substituted Derivatives of the Allylamine Antimycotic Terbinafine. *J. Med. Chem.* **1993**, *36*, 2810−2816.

(9) Nussbaumer, P.; Leitner, I.; Stutz, A. Synthesis of Structure−Activity Relationships of the Novel Homopropargylamine Antimycotics. *J. Med. Chem.* **1994**, *37*, 610−615.

(10) Nussbaumer, P.; Leitner, I.; Mraz, K.; Stutz, A. Synthesis and Structure−Activity Relationships of Side-Chain Substituted Analogues of the Allylamine Antimycotic Terbinafine Lacking the Central Amino Function. *J. Med. Chem.* **1995**, *38*, 1831−1836.

(11) Cramer, R. D.; Patterson, D. E.; Bunce, J. D. Comparative Molecular Field Analysis (CoMFA). 1. Effect of Shape on Binding of Steroids to Carrier Proteins. *J. Am. Chem. Soc.* **1988**, *110*, 5959−5967.

(12) Klebe, G.; Abraham, U. On the Prediction of Binding Properties of Drug Molecules by Comparative Molecular Field Analysis. *J. Med. Chem.* **1993**, *36*, 70−80.

(13) Waller, C. L.; Marshall, G. R. Three-Dimensional Quantitative Structure−Activity Relationship of Angiotensin Converting Enzyme and Thermolysin Inhibitors. II. A Comparison of CoMFA Models Incorporating Molecular Orbital Fields and Desolvation Free Energies Based on Active-Analogue and Complementary-Receptor-Field Alignment Rules. *J. Med. Chem.* **1993**, *36*, 2390−2403.

(14) Depriest, S. A.; Mayer, D.; Naylor, C. B.; Marshall, G. R. 3D-QSAR of Angiotensin-Converting Enzyme and Thermolysin inhibitors: A Comparison of CoMFA Models Based on Deduced and Experimentally Determined Active Site Geometries. *J. Am. Chem. Soc.* **1993**, *115*, 5372−5384.

(15) Waller, C. L.; Oprea, T. I.; Gliotti, A.; Marshall, G. R. Three-Dimensional QSAR of Human Immunodeficiency Virus (I) Protease Inhibitors. 1. A CoMFA Study Employing Experimentally Determined Alignment Rules. *J. Med. Chem.* **1993**, *36*, 4152−4160.

(16) Raghavan, K.; Buolawmini, J. K.; Fesen, M.; Pommier, Y.; Kohn, K. W.; Weinstein, J. N. Three-Dimensional Quantitative Structure Activity Relationship (QSAR) of HIV Integrase Inhibitors: A Comparative Molecular Field Analysis Study. *J. Med. Chem.* **1995**, *38*, 890−897.

(17) Tong, W.; Collantes, E. R.; Chen, Y.; Welsh, W. J. A Comparative Molecular Field Analysis Study of N-Benzylpiperidines as Acetylcholinesterase Inhibitors. *J. Med. Chem.* **1996**, *39*, 380−387.

(18) Cho, S. J.; Garsia, M. L. S.; Bier, J.; Tropsha, A. Structure-Based Alignment and Comparative Molecular Field Analysis of Acetylcholinesterase Inhibitors. *J. Med. Chem.* **1996**, *39*, 5064−5071.

(19) Ortiz, A. R.; Pastor, M.; Palomer, A.; Cruciani, G.; Gago, F.; Wade, R. C. Reliability of Comparative Molecular Field Analysis Models: Effects of Data Scaling and Variable Selection Using a Set of Human Synovial Fluid Phospholipase A_2 Inhibitors. *J. Med. Chem.* **1997**, *40*, 1136−1148.

(20) Carrigan, S. W.; Fox, P. C.; Wall, M. E.; Wani, M. C.; Bowen, P. J. Comparative Molecular Field Analysis and Molecular Modeling Studies of 20-(S)-Camptothecin Analogues as Inhibitors of DNA topoisomerase I and Anticancer/antitumor Agents. *J. Comput.-Aided Mol. Des.* **1997**, *11*, 71−78.

(21) Kulkarni, S. S.; Kulkarni, V. M. Three-Dimensional Quantitative Structure Activity Relationship of Interleukin-1β Converting Enzyme Inhibitors: A Comparative Molecular Field Analysis Study. *J. Med. Chem.* **1999**, *42*, 373−380.

(22) Loghney, D. A.; Schwender, C. F. A Comparison of Progestin and Androgen Binding using the CoMFA technique. *J. Comput.-Aided Mol. Des.* **1992**, *6*, 569−581.

(23) Allen, M. S.; LaLoggia, A. J.; Dorn, L. J.; Martin, M. J.; Constatino, G.; Hagen, T. J.; Koehler, K. F.; Skolnick, P.; Cook, J. M. Predictive Binding of β-Carboline Inverse Agonists and Antagonists via CoMFA/GOLPE Approach. *J. Med. Chem.* **1992**, *35*, 4001−4010.

(24) Krystek, S. R.; Hunt, J. T.; Stein, P. D.; Stouch, T. R. Three-Dimensional Quantitative Structure Activity Relationship of Sulfonamide Endothelin Inhibitors. *J. Med. Chem.* **1995**, *38*, 659−668.

(25) Sicsic, S.; Serraz, I.; Andrieux, J.; Bremont, B.; Allanmant, M. M.; Poncet, A.; Shen, S.; Langlois, M. Three-Dimensional Quantitative Structure−Activity Relaionship of Melatonin Receptor Ligands: A Comparative Molecular Field Analysis Study. *J. Med. Chem.* **1997**, *40*, 739−748.

(26) Moro, S.; Rhee, A. M.; Sanders, L. H.; Jacobson, K. A. Flavonoid Derivatives as Adenosine Receptor Antagonists: A Comparison of the Hypothetical Receptor Binding Site Based on a Comparative Molecular Field Analysis Model. *J. Med. Chem.* **1998**, *41*, 46−52.

(27) Corelli, F.; Manetti, F.; Tafi, A.; Campiani, G.; Nacci, V.; Botta, M. Diltiazem-like Calcium Entry Blockers. A Hypothesis of the Receptor-Binding Site Based on a Comparative Molecular Field Analysis Model. *J. Med. Chem.* **1997**, *40*, 125−131.

(28) Bjokroth, J. P.; Pakkanen, T. A.; Lindroos, J.; Pohjala, E.; Hanhijarvi, H.; Lauren, L.; Hannuniemi, R.; Juhakoski, A.; Kippo, J. K.; Kleimola, T. Comparative Molecular Field Analysis of Clodronic Acid Esters. *J. Med. Chem.* **1991**, *34*, 2338−2343.

(29) McFarland, J. W. Comparative Molecular Field Analysis of Anticoccidial Triazines. *J. Med. Chem.* **1992**, *35*, 2543−2550.

(30) Horwitz, J. P.; Massova, I.; Wiese, T. E.; Wozniak, A. J.; Corbett, T. H.; Seabolt-Leopold, J. S.; Capps, D. B.; Leopold, W. R. Comparative Molecular Field Analysis of in Vitro Growth Inhibition of L1210 and HCT-8 Cells by Some Pyrazoloacridines. *J. Med. Chem.* **1993**, *36*, 3511−3516.

(31) Gamper, A. M.; Winger, R. H.; Liedl, K. R.; Sotriffer, C. A.; Varga, J. M.; Kroemer, R. T.; Rode, B. M. Comparative Molecular Field Analysis of Haptens Docked to the Multispecific Antibody IgE (Lb4). *J. Med. Chem.* **1996**, *39*, 3882−3888.

(32) Diana, G. D.; Kowalczyk, P.; Treasurywala, A. M.; Oglesby, R. C.; Pevear, D. C.; Dutko, F. J. CoMFA Analysis of the Interaction of Antipicornavirus Compounds in the Binding Pocket of Human Rhinovirus-14. *J. Med. Chem.* **1992**, *35*, 1002−1008.

(33) Martinez, A.; Ochoa, C.; Rodriguez, J.; Rodriguez, M.; Castro, A.; Gonzalez, M.; Martinez, M. M. Comparative Molecular Field Analysis (CoMFA) on [6] + [6] Fused Pyrazines with Nematocide Properties. *Quant. Struct. −Act. Relat.* **1997**, *16*, 372−376.

(34) Kroemer, R. T.; Koutsilieri, E.; Hecht, P.; Liedl, K. R.; Riederer, P.; Kornhuber, J. Quantitative Analysis of the Structural Requirements for Blockade of the *N*-Methyl D-aspartate Receptor at the Phencyclidine Binding Site. *J. Med. Chem.* **1998**, *41*, 393−400.

(35) Hecht, P.; Vylpel, H.; Nussbaumer, P.; Berner, H. A Combined Use of Quantum Chemical Parameters, Hydrophobic and Geometrical Descriptors to Establish QSARs of Allylamine Antimycotics. *Quant. Struct.-Act. Relat.* **1992**, *11*, 339−347.

(36) SYBYL 6.22 is available from Tripos Associates Inc., Hanley Road, St. Louis, MO 63144-2913.

(37) Clark, M.; Cramer, R. D., III; Van Opdenbosh, N. Validation of the General-Purpose Tripos 5.2 force field. *J. Comput. Chem.* **1989**, *10*, 982−1012.

(38) Dewar, M. J. S.; Zoebisch, E. G.; Healy, E. G.; Stewart, J. J. P. AM1: A New General Purpose Quantum Mechanical Molecular Model. *J. Am. Chem. Soc.* **1985**, *107*, 3902−3909.

(39) Dewar, M. J. S.; Thiel, W. Ground State of Molecules: 38 The MNDO Method. Approximations and Parameters. *J. Am. Chem. Soc.* **1977**, *99*, 4899−4915.
(40) MOPAC 6.00 is available from Quantum Chemical Program Exchange, Indiana University, no. 455.
(41) Cerius2 3.5 is available from Molecular Simulation Inc., Scranton Road, San Diego, CA.
(42) ClogP version 1.0.0; Biobyte Corp., 201 West 4th Street, Suite 204, Claremount, CA 91711.
(43) Kaminski, J. J.; Doweyko, A. M. Antiulcer Agents 6. Analysis of the in vitro Biochemical and in vivo Gastric Antisecretory Activity of Substituted Imidazo[1,2-α]pyridines and Related Analogues Using Comparative Molecular Field Analysis and Hypothetical Active Site Lattice Methodologies. *J. Med. Chem.* **1997**, *40*, 427−436.

JM9806852